

Complexity and action for warped AdS black holes

Roberto Auzzi^{a,b}, Stefano Baiguera^c, Matteo Grassi^a,
Giuseppe Nardelli^{a,d} and Nicolò Zenoni^a

^a *Dipartimento di Matematica e Fisica, Università Cattolica del Sacro Cuore,
Via Musei 41, 25121 Brescia, Italy*

^b *INFN Sezione di Perugia, Via A. Pascoli, 06123 Perugia, Italy*

^c *Università degli studi di Milano Bicocca and INFN, Sezione di Milano - Bicocca,
Piazza della Scienza 3, 20161, Milano, Italy*

^d *TIFPA - INFN, c/o Dipartimento di Fisica, Università di Trento,
38123 Povo (TN), Italy*

E-mails: roberto.auzzi@unicatt.it, s.baiguera@campus.unimib.it,
matteogr@gmail.com, giuseppe.nardelli@unicatt.it,
zenon94@hotmail.it

Abstract

The Complexity=Action conjecture is studied for black holes in Warped AdS₃ space, realized as solutions of Einstein gravity plus matter. The time dependence of the action of the Wheeler-DeWitt patch is investigated, both for the non-rotating and the rotating case. The asymptotic growth rate is found to be equal to the Hawking temperature times the Bekenstein-Hawking entropy; this is in agreement with a previous calculation done using the Complexity=Volume conjecture.

1 Introduction

The AdS/CFT correspondence gives us a non-perturbative formulation of quantum gravity for a class of spacetimes with negative curvature and AdS asymptotic. Despite many evidences for the validity of the correspondence, it would be desirable to improve our understanding about how the spacetime geometry emerges out of the quantum field theory degrees of freedom living in the boundary. Quantum information concepts seem somehow to encode non trivial geometric properties of the gravitational theory in the bulk. For example, the area of minimal surface in AdS is dual to the entanglement entropy of the boundary subregion [1, 2, 3]. However, the precise mechanism by which the dual bulk spacetime geometry emerges out of the boundary quantum field theory is still not understood.

Entropy is a crucial quantity in order to describe classical and quantum aspects [4, 5] of Black Holes (BHs). However, it does not seem the right dual quantity in order to describe the Einstein-Rosen Bridge (ERB) in the interior of a two-sided Kruskal BH. In the AdS/CFT correspondence, a two sided eternal BH is dual to a thermofield doublet state, in which the two conformal field theories living on the left and right boundaries are entangled [6]. Taking the two boundary times going in the same direction, this entangled state is time-dependent [7], and the geometry of the ERB connecting the two sides grows linearly with time. The ERB continues to grow for a much longer timescale compared to the thermalization time, and so entropy does not provide us with a good dual quantity for this process.

Motivated by the need to find a boundary dual to such behavior, recently a new quantum information tool has joined the discussion: computational complexity [8, 9]. For a quantum-mechanical system, it is defined as the minimal number of basic unitary operation which are needed in order to prepare a given state starting from a simple reference state. A proper definition of complexity in quantum field theory has several subtleties, including the choice of the reference state and of the allowed set of elementary quantum gates and the allowed amount of tolerance which is introduced in order to specify the accuracy with which the state should be produced. Recently, concrete calculations have been performed in the case of free field theories [10, 11, 12]. Another interesting approach to complexity [13, 14] in quantum field theory uses tensor networks [15] in connection with the Liouville action.

Two different gravity dual of the quantum complexity of a state have been proposed so far: the complexity=volume (CV) [8, 9, 16] and the complexity=action (CA) [17, 18] conjectures. In the CV conjecture, complexity is proportional to the volume V of a maximal codimension one sub-manifold hanging from the boundary. In the CA conjecture, complexity \mathcal{C} is proportional to the action I evaluated in the causal diamond of a boundary section at constant time, which is called Wheeler-DeWitt (WDW) patch:

$$\mathcal{C} = \frac{I}{\pi\hbar}, \quad (1.1)$$

In this case the action has several contributions beyond the traditional bulk Einstein-Hilbert (EH) and boundary Gibbons-Hawking-York (GHY) terms: in particular surface joint contributions [19, 20] turn out to be important in order to compute the full time dependence of the WDW action [20, 21, 22]. Moreover, ambiguities due to contributions to the action from null surfaces [23, 24] are also present; these ambiguities do not affect the late-time limit of complexity, which can be computed just from the EH and GHY terms in the action [17, 18].

The CA and CV conjectures have been recently investigated in several AdS/CFT settings: for example for rotating/charged BHs in several dimensions [25], for spacetime singularities [26, 27], for the soliton [28], in the Vaidya spacetime [29, 30, 31, 32] and in theories with dilatons [33, 34].

Quantum information has been rather extensively studied for asymptotically AdS spacetimes; the understanding that we have for other spacetimes, such as the asymptotically flat or the de Sitter, is much more limited, because we have so far very little clues about the dual field theory, if it exists. An interesting ultraviolet deformation of AdS/CFT where we have a good amount of information about the structure of the field theory dual is the Warped AdS₃/CFT₂ correspondence [35, 36, 37, 38]. This is a duality between gravitational theories in 2 + 1 dimensions in a space with Warped AdS₃ asymptotic and a conjectured class of non-relativistic theories in 1 + 1 dimensions, called Warped Conformal Field Theories (WCFTs), whose symmetry content includes a copy of the Virasoro and of the $U(1)$ Kac-Moody current algebras. Recently, several progresses have been made in order to put this duality on firmer grounds; for example, an analog of Cardy formula was derived in [36]. The issue of entanglement entropy was studied by several authors, e.g. [39, 40, 41, 42, 43]. The CV conjecture was recently studied in [44]; in this paper we will instead address the CA conjecture.

The paper is organized as follows: in section 2 we review general properties of BHs in WAdS space, realized as a solution of Einstein gravity plus matter, and we discuss the null coordinates needed to define the WDW patch. In section 3 we consider the various contributions to the action, following the approach of [20]. In section 4 we compute the action for both the non-rotating and rotating case. We conclude in section 5. Technical details about the matching with the metric of [45] are discussed in appendix A. An alternative calculation using the approach of [18] is presented in appendix B: this is valid just in the late-time limit and agrees with the more general calculation presented in section 4.

2 Warped Black Holes in Einstein gravity

We consider the following class of BHs with Warped AdS₃ asymptotic [46, 47, 35]:

$$\frac{ds^2}{l^2} = dt^2 + \frac{dr^2}{(\nu^2 + 3)(r - r_+)(r - r_-)} + \left(2\nu r - \sqrt{r_+ r_- (\nu^2 + 3)}\right) dt d\theta + \frac{r}{4} \Psi d\theta^2, \quad (2.1)$$

$$\Psi(r) = 3(\nu^2 - 1)r + (\nu^2 + 3)(r_+ + r_-) - 4\nu\sqrt{r_+ r_- (\nu^2 + 3)}. \quad (2.2)$$

We introduce \tilde{r}_0 as

$$\tilde{r}_0 = \max(0, \rho_0), \quad \rho_0 = \frac{4\nu\sqrt{r_+ r_- (\nu^2 + 3)} - (\nu^2 + 3)(r_+ + r_-)}{3(\nu^2 - 1)}, \quad (2.3)$$

where $\Psi(\rho_0) = 0$ and we take the range of variables as follows: $\tilde{r}_0 \leq r < \infty$, $-\infty < t < \infty$, $\theta \sim \theta + 2\pi$ and the horizons are located at $r = r_+, r_-$ with $r_+ \geq r_-$. These metrics can be obtained by discrete quotients of WAdS₃ [35]; we take $\nu \geq 1$ in order to avoid closed time-like curves. For $\nu = 1$ the metric (2.1) reduces to the the Banados-Teitelboim-Zanelli (BTZ) black hole [48, 49]. The warping parameter ν is related in the holographic dictionary to the left and right central charges of the boundary WCFT, which for Einstein gravity are [50]:

$$c_L = c_R = \frac{12l\nu^2}{G(\nu^2 + 3)^{3/2}}. \quad (2.4)$$

Temperature and angular velocity of horizon are [35]:

$$T = \frac{\nu^2 + 3}{4\pi l} \frac{r_+ - r_-}{2\nu r_+ - \sqrt{(\nu^2 + 3)r_+ r_-}}, \quad \Omega = \frac{2}{(2\nu r_+ - \sqrt{(\nu^2 + 3)r_+ r_-})l}. \quad (2.5)$$

The metric (2.1) can be obtained as a vacuum solution of Topologically Massive Gravity (TMG) [46, 47], New Massive Gravity (NMG) [51], general linear combinations of the two

mass terms [52] and also in string theory constructions [53, 54, 55]. We will be interested to WAdS₃ BHs realized as solution of Einstein gravity with matter. Unfortunately, all the known realizations of WAdS₃ BHs in Einstein gravity have some pathology in the matter content: for example, they can be realized as solutions with perfect fluid stress tensor with spacelike quadrivelocity [56].

We will use for concreteness the model studied in [45, 57], which is Chern-Simons-Maxwell electrodynamics coupled to Einstein gravity. In order to have solutions without closed time-like curves, a wrong sign for the kinetic Maxwell term is needed. Solutions with positive Maxwell kinetic energy have $\nu^2 < 1$ and correspond to Gödel spacetimes. We will see that the CA conjecture is so solid that can survive to unphysical action with ghosts.

In the Einstein gravity case the entropy is given by the area of the horizon:

$$S = \frac{l\pi}{4G}(2\nu r_+ - \sqrt{r_+ r_- (\nu^2 + 3)}). \quad (2.6)$$

and the conserved charges (mass and angular momentum) are [45, 57, 44]:

$$M = \frac{1}{16G}(\nu^2 + 3) \left((r_- + r_+) - \frac{\sqrt{r_+ r_- (\nu^2 + 3)}}{\nu} \right), \quad (2.7)$$

$$J = \frac{l}{32G}(\nu^2 + 3) \left(\frac{r_- r_+ (3 + 5\nu^2)}{2\nu} - (r_+ + r_-) \sqrt{(3 + \nu^2) r_+ r_-} \right). \quad (2.8)$$

2.1 Null coordinates

The expression of the metric (2.1) in Arnowitt-Deser-Misner (ADM) form is:

$$ds^2 = -N^2 dt^2 + \frac{l^4 dr^2}{4R^2 N^2} + l^2 R^2 (d\theta + N^\theta dt)^2, \quad (2.9)$$

where

$$R^2 = \frac{r}{4}\Psi, \quad N^2 = \frac{l^2(\nu^2 + 3)(r - r_+)(r - r_-)}{4R^2}, \quad N^\theta = \frac{2\nu r - \sqrt{r_+ r_- (\nu^2 + 3)}}{2R^2}. \quad (2.10)$$

It is useful to use a set of null coordinates which delimit the WDW patch. These coordinates were introduced in [58]. We consider a set of null geodesics which satisfy $(d\theta + N^\theta dt) = 0$; then a positive-definite term in the metric (2.9) saturates to zero, and the null geodesics are given by the constant u and v trajectories:

$$du = dt - \frac{l^2}{2RN^2} dr, \quad dv = dt + \frac{l^2}{2RN^2} dr. \quad (2.11)$$

The normal one-forms to the WDW null surfaces are given by du and dv ; we introduce two vectors v_α, u_α such that

$$dv = v_\alpha dx^\alpha, \quad du = u_\alpha dx^\alpha, \quad (2.12)$$

which are normal and tangent to the null surfaces which delimit the WDW patch. The corresponding Eddington-Finkelstein coordinates then are:

$$u = t - r^*(r), \quad v = t + r^*(r), \quad (2.13)$$

where

$$\frac{dr^*}{dr} = \frac{l^2}{2RN^2} = \frac{\sqrt{r\Psi(r)}}{(\nu^2 + 3)(r - r_-)(r - r_+)}. \quad (2.14)$$

The non-rotating case is defined by the condition $J = 0$, and corresponds to the following values:

$$r_- = 0, \quad \frac{r_+}{r_-} = \frac{4\nu^2}{\nu^2 + 3}. \quad (2.15)$$

In this case the Penrose diagram is the same as the ones for the Schwarzschild BH in four dimension [58]. In the rotating case, for generic (r_+, r_-) , the Penrose diagram is the same as the one of the Reissner-Nordström BH.

2.2 An explicit model

In this section we consider an explicit Einstein gravity model which admits the metric eq. (2.1) as a solution [45]. The matter content is a gauge field with Chern-Simons and Maxwell terms, and the bulk part of the action is:

$$I_{\mathcal{V}} = \frac{1}{16\pi G} \int d^3x \left\{ \sqrt{g} \left[\left(R + \frac{2}{L^2} \right) - \frac{\kappa}{4} F^{\mu\nu} F_{\mu\nu} \right] - \frac{\alpha}{2} \epsilon^{\mu\nu\rho} A_\mu F_{\nu\rho} \right\} = \int d^3x \sqrt{g} \mathcal{S}, \quad (2.16)$$

where $\epsilon^{\mu\nu\rho}$ is the Levi-Civita tensorial density. Here we put a coefficient $\kappa = \pm 1$ in front of the Maxwell kinetic term.

The equations of motion for the gauge field are

$$D_\mu F^{\alpha\mu} = -\frac{\alpha}{\kappa} \frac{\epsilon^{\alpha\nu\rho}}{\sqrt{g}} F_{\nu\rho}, \quad (2.17)$$

while the Einstein equations are

$$G_{\mu\nu} - \frac{1}{L^2} g_{\mu\nu} = \frac{\kappa}{2} T_{\mu\nu}, \quad T_{\mu\nu} = F_{\mu\alpha} F_\nu^\alpha - \frac{1}{4} g_{\mu\nu} F^{\alpha\beta} F_{\alpha\beta}. \quad (2.18)$$

We consider the set of coordinates (r, t, θ) where the metric assumes the form (2.1), and we choose a gauge motivated by the ansatz from [45]:

$$A =adt + (b + cr)d\theta, \quad F = c dr \wedge d\theta, \quad (2.19)$$

where $\{a, b, c\}$ is a set of constants. Thus, the Maxwell equations give:

$$\alpha = \kappa \frac{\nu}{l}. \quad (2.20)$$

From the Einstein equations, we get, independently from (r_+, r_-) :

$$L = l \sqrt{\frac{2}{3 - \nu^2}}, \quad c = \pm l \sqrt{\frac{3}{2} \frac{1 - \nu^2}{\kappa}}. \quad (2.21)$$

There is conflict between absence of closed time-like curves and presence of ghosts ($\kappa = -1$).

Note that the parameters a, b are not constrained by the equations of motion; the action itself does not depend on the parameter b , but it depends explicitly on the gauge parameter a through the Chern-Simons term. This parameter is important in order to properly define the conserved charge which gives the mass M [57]. Only for a particular value of a the mass is indeed associated to the Killing vector $\partial/\partial t$ and is independent from the $U(1)$ gauge transformations. This corresponds to the $\zeta = 0$ gauge in [45]; in our notation it corresponds to:

$$A_t = a = \frac{l}{\nu} \sqrt{\frac{3}{2}} \sqrt{\nu^2 - 1}. \quad (2.22)$$

The comparison with the solution of [45] is discussed in appendix A.

3 Evaluating the action

The action in the WDW patch has several contributions:

$$I = I_{\mathcal{V}} + I_{\mathcal{B}} + I_{\mathcal{J}}, \quad (3.1)$$

where $I_{\mathcal{V}}$ is the bulk contribution (see eq. (2.16)), $I_{\mathcal{B}}$ the the boundary term and $I_{\mathcal{J}}$ the joint term studied in detail in [20].

The bulk action integrand $\sqrt{g}\mathcal{S}$ in eq. (2.16) evaluated on the background (2.1) and (2.19) is constant and independent from the parameters (r_+, r_-) :

$$I_{\mathcal{V}} = \int dr dt d\theta \frac{\mathcal{I}}{16\pi G}, \quad \mathcal{I} = -\frac{l}{2}(\nu^2 + 3) + \frac{\kappa c^2}{l} - \alpha a c. \quad (3.2)$$

The boundary terms can be written as:

$$I_{\mathcal{B}} = I_{\text{GHY}} + I_{\mathcal{N}}, \quad (3.3)$$

where I_{GHY} is the contribution for spacelike and timelike boundaries (Gibbons-Hawking-York (GHY) term) and $I_{\mathcal{N}}$ is the contribution for null boundaries. The GHY term is:

$$I_{\text{GHY}} = \frac{\varepsilon}{8\pi G} \int_{\mathcal{B}} d^2x \sqrt{|h|} K, \quad (3.4)$$

where \mathcal{B} is the appropriate boundary, h the induced metric, K the extrinsic curvature and ε is equal to $+1$ if the boundary is timelike and -1 if it is spacelike. For null surface boundaries the contribution to the action is [23, 24, 20]

$$I_{\mathcal{N}} = \frac{1}{8\pi G} \int_{\mathcal{B}} \tilde{\kappa} d\lambda dS, \quad (3.5)$$

where λ parameterizes the null direction of the surface, dS is the area element of the spatial cross-section orthogonal to the null direction and $\tilde{\kappa}$ measures the failure of λ to be an affine parameter: if we denote by k^α the null generator, $\tilde{\kappa}$ is defined by the relation: $k^\mu D_\mu k^\alpha = \tilde{\kappa} k^\alpha$. It turns out that the contribution to the action $I_{\mathcal{N}}$ is not parameterization-invariant [24, 20] and it can be set to zero using an affine parameterization for the null direction of the boundary [20].

In the case of joints between spacelike and timelike surfaces, this contribution was studied in [19]. The analysis for joints between null and timelike, spacelike or another null surface were recently studied in [20]. In the CA calculations done in the next sections, we will use these null joints contributions several times:

$$I_{\mathcal{J}} = \frac{1}{8\pi G} \int_{\Sigma} d\theta \sqrt{\sigma} \mathbf{a}, \quad (3.6)$$

where σ_{ab} is the induced metric over the joint (in this case, it is 1-dimensional) and \mathbf{a} depends on the kind of joint. Let us denote k^α the future directed null normal to a null surface (which is also tangent to the surface), n_α the normal to a spacelike surface and s_α the normal to a timelike surface, both directed outwards the volume of interest. In the case of intersection of two null surfaces with normals k_1^α and k_2^α :

$$\mathbf{a} = \eta \log \left| \frac{k_1 \cdot k_2}{2} \right|, \quad (3.7)$$

while in the case of intersection of a null surface with normal k^α and a spacelike surface with normal n^α (or a timelike surface with normal s^α):

$$\mathbf{a} = \eta \log |k \cdot n|, \quad \mathbf{a} = \eta \log |k \cdot s|. \quad (3.8)$$

In eqs. (3.7-3.8) we should set $\eta = +1$ if the joint lies in past of the spacetime volume of interest, and $\eta = -1$ if the joint lies in the future of the relevant region. Note that eqs. (3.7) and (3.8) are slightly ambiguous because the normalization of a null normal k^α is ambiguous. This ambiguity is related to the one due to the null surfaces and does not affect the late-time limit of the complexity, but just the finite-time behavior¹. As discussed in [22], we will partially fix this ambiguity by requiring that the null vector k^μ have constant scalar product with the boundary time killing vector $\partial/\partial t$.

4 Complexity=Action

The Penrose diagram for the non-rotating case is shown in figure 1, with some lines at constant r and t . Both in the rotating and non-rotating cases, for $r \rightarrow \infty$, the asymptotic behavior of $r^*(r)$ is

$$r^*(r) \approx \frac{3\sqrt{\nu^2 - 1}}{\nu^2 + 3} \log r \equiv C \log r. \quad (4.1)$$

So we should first fix a cutoff surface at $r = \Lambda$ to make our calculations finite. The WDW surface is bounded by lines with constant values of v and u , which in the Penrose diagram correspond to 45 degrees lines.

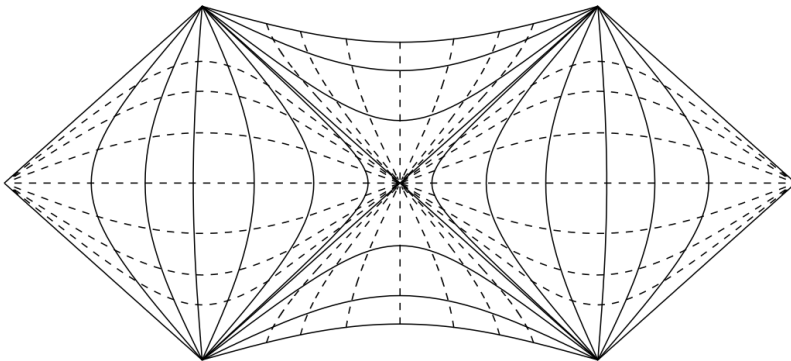


Figure 1: Constant r lines (solid) and constant t lines (dashed) of the Penrose diagram in the non-rotating case.

On the left and right boundaries, the time coordinate t diverges to $\pm\infty$ in the upper and lower sides, respectively. From eqs. (2.13), a change of cutoff from Λ_1 to Λ_2 , implies a constant shift in the time coordinate by $C \log \frac{\Lambda_2}{\Lambda_1}$. For $\nu = 1$ we recover the AdS asymptotic, $r^*(\infty)$ is finite and no shift is needed; the Penrose diagram in this case is different and is the standard one of the BTZ black hole.

The BH has a left and a right boundary, where two identical copies of a dual entangled WCFT live. To avoid divergences, the times at the left and right boundaries are evaluated at the cutoff surface $r = \Lambda$, and are respectively denoted by t_L and t_R . If we take the two times going in opposite directions:

$$t_L \rightarrow t_L + \Delta t, \quad t_R \rightarrow t_R - \Delta t, \quad (4.2)$$

¹These ambiguities could be related to various ambiguities of the dual circuit complexity of the quantum state, such as the choice of the reference state, the specific set of elementary gates and the amount of tolerance that one introduces to describe the accuracy with which the final state should be constructed.

the entangled thermofield doublet is time-independent, because this time shift corresponds to the time Killing vector of the BH solution. If instead we take the two boundary times going in the same direction, i.e.

$$t_L \rightarrow t_L + \Delta t, \quad t_R \rightarrow t_R + \Delta t, \quad (4.3)$$

the BH solution is dual to a time-dependent thermofield doublet [7]:

$$|\Psi_{TFD}\rangle \propto \sum_n e^{-E_n\beta/2 - iE_n(t_L+t_R)} |E_n\rangle_R |E_n\rangle_L. \quad (4.4)$$

where $|E_n\rangle_{L,R}$ denotes the energy eigenstates of left and right boundary theories and β is the inverse temperature. Without loss of generality, we can choose

$$t_L = t_R = \frac{t_b}{2}. \quad (4.5)$$

4.1 Non-rotating case

The non-rotating case corresponds to the values in eq. (2.15); for simplicity we focus just on $r_- = 0$ and we set $r_+ = r_0$. The analysis for the other value of r_+/r_- in eq. (2.15) is analogous: it can be shown that it can be mapped to $r_- = 0$ by a change of variables [58]. The Penrose diagrams for the non-rotating case are shown in figures 2 and 3.

The structure of the WDW patch in the non-rotating case changes with time; at early times it looks like in figure 2, while at late times like in figure 3. In particular, there exists a critical time t_C such that the bottom vertex of the patch touches the past singularity. The critical time is given by

$$t_C = 2(r_\Lambda^* - r^*(0)), \quad (4.6)$$

where $r_\Lambda^* = r^*(\Lambda)$. We will separate the calculation of the action in two cases. At the end we will express the results in terms of

$$\tau = l(t_b - t_C), \quad (4.7)$$

where τ is the boundary time rescaled with curvature l for dimensional purposes and with the origin translated at the critical time t_C .

4.1.1 Initial times $t_b < t_C$

Bulk contributions: We decompose the WDW patch into three regions and we use the symmetry of the configuration to write the bulk action as

$$I_{\mathcal{V}} = 2 (I_{\mathcal{V}}^1 + I_{\mathcal{V}}^2 + I_{\mathcal{V}}^3), \quad (4.8)$$

where

$$\begin{aligned} I_{\mathcal{V}}^1 &= \frac{\mathcal{I}}{16\pi G} \int_0^{2\pi} d\theta \int_{\varepsilon_0}^{r_0} dr \int_0^{v-r^*(r)} dt = \frac{\mathcal{I}}{8G} \int_{\varepsilon_0}^{r_0} dr \left(\frac{t_b}{2} + r_\Lambda^* - r^*(r) \right), \\ I_{\mathcal{V}}^2 &= \frac{\mathcal{I}}{16\pi G} \int_0^{2\pi} d\theta \int_{r_0}^{\Lambda} dr \int_{u+r^*(r)}^{v-r^*(r)} dt = \frac{\mathcal{I}}{4G} \int_{r_0}^{\Lambda} dr (r_\Lambda^* - r^*(r)), \\ I_{\mathcal{V}}^3 &= \frac{\mathcal{I}}{16\pi G} \int_0^{2\pi} d\theta \int_{\varepsilon_0}^{r_0} dr \int_{u+r^*(r)}^0 dt = \frac{\mathcal{I}}{8G} \int_{\varepsilon_0}^{r_0} dr \left(-\frac{t_b}{2} + r_\Lambda^* - r^*(r) \right). \end{aligned} \quad (4.9)$$

Summing all the contributions, we get the result

$$I_{\mathcal{V}} = \frac{\mathcal{I}}{2G} \int_{\varepsilon_0}^{\Lambda} dr (r_\Lambda^* - r^*(r)) \equiv I_{\mathcal{V}}^0. \quad (4.10)$$

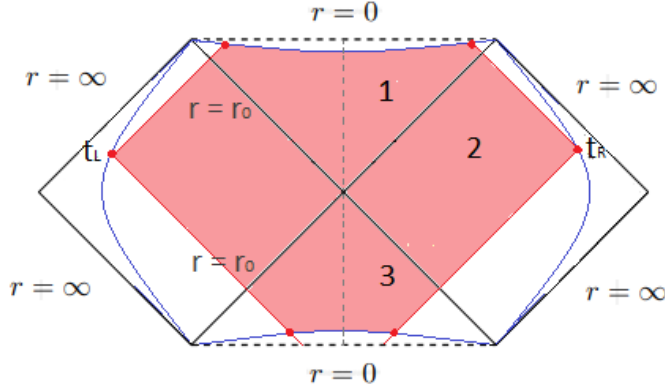


Figure 2: Penrose diagram for the non-rotating BH, with the WDW patch for $t_b < t_C$.

This contribution is time-independent.

GHY surface contributions: The constant r surface, inside the horizon, is a spacelike surface whose induced metric in the $x^i = (t, \theta)$ coordinates reads:

$$h_{ij} = l^2 \begin{pmatrix} 1 & \nu r \\ \nu r & \frac{r}{4} \Psi(r) \end{pmatrix}, \quad \sqrt{h} = \frac{l^2}{2} \sqrt{(\nu^2 + 3)r(r_0 - r)}. \quad (4.11)$$

The normal vector to these slices is

$$n^\mu = \left(0, -\frac{1}{l} \sqrt{(\nu^2 + 3)r(r_0 - r)}, 0 \right), \quad n^\alpha n_\alpha = -1, \quad (4.12)$$

and the extrinsic curvature is

$$K = \frac{1}{2l} \sqrt{\nu^2 + 3} \frac{2r - r_0}{\sqrt{r(r_0 - r)}}. \quad (4.13)$$

In the GHY we should then use $\varepsilon = -1$ because the surface is spacelike. We are now able to compute the two contributions to the GHY term coming from the regions near the past and future singularities:

$$I_{\text{GHY}}^1 = -\frac{(\nu^2 + 3)l}{16G} \left[(2r - r_0) \left(\frac{t_b}{2} + r_\Lambda^* - r^*(r) \right) \right]_{r=\varepsilon_0}, \quad (4.14)$$

$$I_{\text{GHY}}^2 = -\frac{(\nu^2 + 3)l}{16G} \left[(2r - r_0) \left(-\frac{t_b}{2} + r_\Lambda^* - r^*(r) \right) \right]_{r=\varepsilon_0}. \quad (4.15)$$

The total GHY contribution then is:

$$I_{\text{GHY}} = 2 (I_{\text{GHY}}^1 + I_{\text{GHY}}^2) = -\frac{(\nu^2 + 3)l}{4G} [(2r - r_0) (r_\Lambda^* - r^*(r))]_{r=\varepsilon_0} \equiv I_{\text{GHY}}^0, \quad (4.16)$$

which is time-independent.

Joint contributions: There are four joints between null and spacelike surfaces at $r = \varepsilon_0$ (nearby the future and past singularities) and two joints at $r = \Lambda$. The normal to the constant r spacelike surfaces is n^α given by eq. (4.12), while the normal to the lightlike surfaces are u^α, v^α from eq. (2.12). From eq. (3.8), the four joint contributions nearby the singularities vanish, while the two joint contribution nearby the UV cutoff are time-independent (see eq. 3.7).

Total: Summing all the terms coming from the bulk, the boundary and the joint contributions, we find that the action of the WDW patch is time-independent.

4.1.2 Later times $t_b > t_C$

After the critical time t_C , the WDW patch moves and the lower vertex of the diagram does not reach the past singularity (see figure 3). This vertex is defined via the relation

$$\frac{t_b}{2} - r_\Lambda^* + r^*(r_m) = 0. \quad (4.17)$$

The evaluation of the null joint contributions will require the computation of the time derivative of the tortoise coordinate, which is done by differentiating eq. (4.17):

$$\frac{dr_m}{dt_b} = -\frac{1}{2} \left(\frac{dr^*(r_m)}{dr_m} \right)^{-1}. \quad (4.18)$$

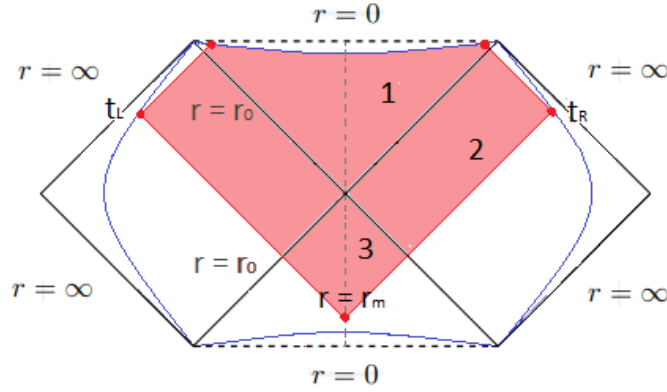


Figure 3: Penrose diagram for the non-rotating BH, with the WDW patch for $t_b > t_C$.

Bulk contributions: The bulk action is the same of the case $t_b < t_C$, apart from the last contribution which becomes

$$I_{\mathcal{V}}^3(t_b > t_C) = \frac{\mathcal{I}}{16\pi G} \int_0^{2\pi} d\theta \int_{r_m}^{r_0} dr \int_{u+r^*(r)}^0 dt = \frac{\mathcal{I}}{8G} \int_{r_m}^{r_0} dr \left(-\frac{t_b}{2} + r_\Lambda^* - r^*(r) \right). \quad (4.19)$$

We can re-write this contribution in the following way:

$$I_{\mathcal{V}}^3(t_b > t_C) = I_{\mathcal{V}}^3(t_b < t_C) + \frac{\mathcal{I}}{8G} \int_{\varepsilon_0}^{r_m} dr \left(\frac{t_b}{2} - r_\Lambda^* + r^*(r) \right). \quad (4.20)$$

Since the other contributions to the bulk action are unchanged, the total result is

$$I_{\mathcal{V}}(t_b > t_C) = I_{\mathcal{V}}^0 + \frac{\mathcal{I}}{4G} \int_{\varepsilon_0}^{r_m} dr \left(\frac{t_b}{2} - r_\Lambda^* + r^*(r) \right), \quad (4.21)$$

the first term being time-independent. The time derivative of the bulk action then is:

$$\frac{dI_{\mathcal{V}}}{dt_b}(t_b > t_C) = \frac{\mathcal{I}}{8G} r_m = \frac{1}{8G} \left[-\frac{l}{2}(\nu^2 + 3) + \frac{\kappa c^2}{l} - \alpha ac \right] r_m, \quad (4.22)$$

where the defining relation (4.17) is used in order to obtain a vanishing contribution from the upper integration extreme.

GHY surface contributions: After the critical time t_C we only have a contribution from the future singularity, because the lower part of the WDW patch does not reach the past singularity. We are only left with

$$I_{\text{GHY}} = 2I_{\text{GHY}}^1 = -\frac{(\nu^2 + 3)l}{8G} \left[(2r - r_0) \left(\frac{t_b}{2} + r_\Lambda^* - r^*(r) \right) \right]_{r=\varepsilon_0}, \quad (4.23)$$

which is time-dependent. The time derivative of this term gives:

$$\lim_{\varepsilon_0 \rightarrow 0} \frac{dI_{\text{GHY}}}{dt_b} (t_b > t_C) = \frac{(\nu^2 + 3)l}{16G} r_0. \quad (4.24)$$

Joint contributions: Following the same procedure of the case $t_b < t_C$, we find that the null joints at the UV cutoff give time-independent contributions, while the joint at the future singularity gives a vanishing result. The contribution from the remaining null-null joint between u^α and v^α at $r = r_m$ is instead time-dependent, because r_m is function of time (see eq. (4.18)). We find that this contribution to the action is given by eq. (3.6), with \mathfrak{a} given by eq. (3.7):

$$\mathfrak{a} = \log \left| A^2 \frac{u^\alpha v_\alpha}{2} \right| = \log \left| A^2 \frac{1}{l^2} \frac{\Psi(r)}{(\nu^2 + 3)(r - r_0)} \right|. \quad (4.25)$$

The normalization factor A^2 corresponds to an ambiguity in the contribution to the action due to the null joint [20], because the normalization of the two null normals u^α and v^α which delimitate the WDW patch is in principle not fixed by the metric (see the discussion at the end of section 3). The action contribution from eq. (4.25), evaluated for $r = r_m$, gives:

$$I_{\mathcal{J}} = -\frac{l}{4G} \sqrt{\frac{r_m}{4} \Psi(r_m)} \log \left| \frac{l^2 (\nu^2 + 3)(r_m - r_0)}{A^2 \Psi(r_m)} \right|, \quad (4.26)$$

whose time derivatives is:

$$\begin{aligned} \frac{dI_{\mathcal{J}}}{dt_b} = & -\frac{l}{16G} \frac{dr_m}{dt_b} \frac{6(\nu^2 - 1)r_m + (\nu^2 + 3)r_0}{\sqrt{r_m [3(\nu^2 - 1)r_m + (\nu^2 + 3)r_0]}} \log \left| \frac{l^2 (\nu^2 + 3)(r_m - r_0)}{A^2 \Psi(r_m)} \right| + \\ & -\frac{l}{8G} \frac{dr_m}{dt_b} \frac{4\nu^2 r_0 \sqrt{r_m [3(\nu^2 - 1)r_m + (\nu^2 + 3)r_0]}}{(r_m - r_0) (3r_m(\nu^2 - 1) + (\nu^2 + 3)r_0)}. \end{aligned} \quad (4.27)$$

Inserting eq. (4.18) we obtain:

$$\begin{aligned} \frac{dI_{\mathcal{J}}}{dt_b} = & \frac{l}{32G} \frac{(\nu^2 + 3)(r_m - r_0) (6(\nu^2 - 1)r_m + (\nu^2 + 3)r_0)}{3(\nu^2 - 1)r_m + (\nu^2 + 3)r_0} \log \left| \frac{l^2 (\nu^2 + 3)(r_m - r_0)}{A^2 \Psi(r_m)} \right| + \\ & + \frac{l}{16G} \frac{4\nu^2 (\nu^2 + 3)r_m r_0}{3r_m(\nu^2 - 1) + (\nu^2 + 3)r_0}. \end{aligned} \quad (4.28)$$

Total: The total time derivative of the action is finally given by

$$\begin{aligned} \frac{dI}{dt_b} = & \frac{1}{8G} \left[-\frac{l}{2} (\nu^2 + 3) + \frac{\kappa c^2}{l} - \alpha ac \right] r_m + \frac{(\nu^2 + 3)l}{16G} r_0 + \frac{l}{16G} \frac{4\nu^2 (\nu^2 + 3)r_m r_0}{3r_m(\nu^2 - 1) + (\nu^2 + 3)r_0} \\ & + \frac{l}{32G} \frac{(\nu^2 + 3)(r_m - r_0) (6(\nu^2 - 1)r_m + (\nu^2 + 3)r_0)}{3(\nu^2 - 1)r_m + (\nu^2 + 3)r_0} \log \left| \frac{l^2 (\nu^2 + 3)(r_m - r_0)}{A^2 \Psi(r_m)} \right|. \end{aligned} \quad (4.29)$$

We can now perform the late time limit of the previous rate. In this limit $r_m \rightarrow r_0$, which implies that the term in the second line vanishes and we find:

$$\lim_{t_b \rightarrow \infty} \frac{dI}{dt_b} = \frac{(\nu^2 + 3)l}{16G} r_0 + \frac{1}{8G} \left(\frac{\kappa}{l} c^2 - \alpha ac \right) r_0. \quad (4.30)$$

Note that the general result (4.29) depends on A^2 , while its late time limit does not. Using the value of a given in eq. (2.22), we can now evaluate the combination appearing in the rate of the action

$$\frac{\kappa}{l}c^2 - \alpha ac = 0. \quad (4.31)$$

We finally obtain:

$$\lim_{t_b \rightarrow \infty} \frac{1}{l} \frac{dI}{dt_b} = \lim_{\tau \rightarrow \infty} \frac{dI}{d\tau} = \frac{\nu^2 + 3}{16G} r_0 = M = TS. \quad (4.32)$$

This late-time results can also be recovered using the approach by [18] (see Appendix B for details).

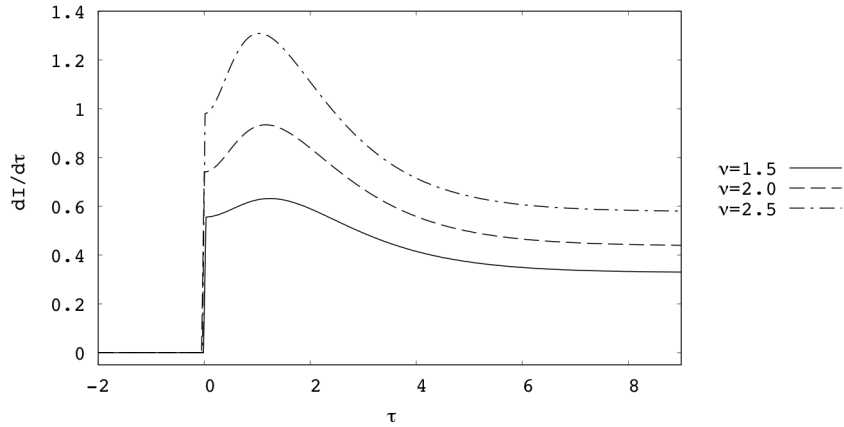


Figure 4: Time dependence of the WDW action in the non-rotating case for different values of ν . We set $G = 1$, $l = 1$, $r_0 = 1$ and $A = 2$. The critical time t_C corresponds to $\tau = 0$.

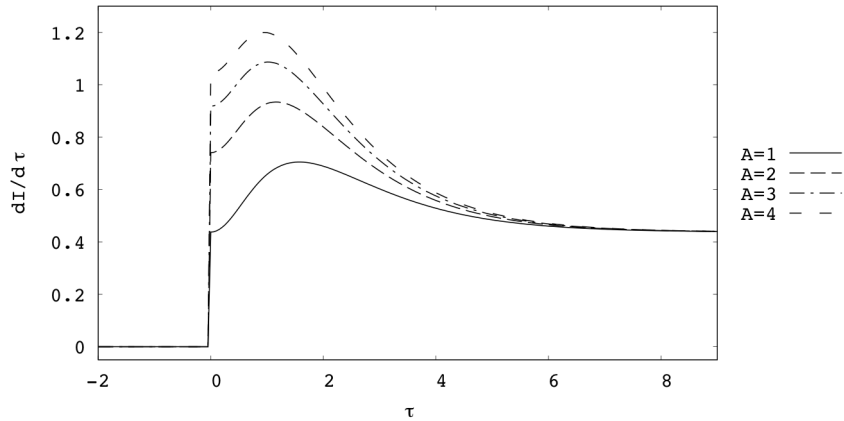


Figure 5: Time dependence of the WDW action in the non-rotating case for different values of the parameter A . We set $G = 1$, $l = 1$, $r_0 = 1$ and $\nu = 2$.

Numerical plots of the time dependence of the action rate (4.29) for different values of ν are shown in figure 4. The same qualitative structure as for the AdS case [22] is found; in particular the growth rate of the action is a decreasing function at late times. As in [22], the late-time limit then overshoots the asymptotic rate, which was previously believed [18] to be associated to an universal upper bound, conjectured by Lloyd [59]. There is some

dependence at finite time on the parameter A , see figure 5; this is a feature also of the AdS case [20, 21, 22]. The late-time limit is instead independent from A .

4.2 Rotating case

In the rotating case (see figure 6) we do not need to distinguish between initial and later times, because in this case the form of the WDW patch is the same at any time and the complexity is already non-vanishing at initial times. We define $\tau = lt_b$. We call r_{m1}, r_{m2} the null joints referring respectively to the top and bottom vertices of the spacetime region of interest. Due to the structure of the Penrose diagram in the rotating case (similar to the 3+1 dimensional diagram for a Reissner-Nordstrom black hole), we do not have boundaries contributing to the GHY term.

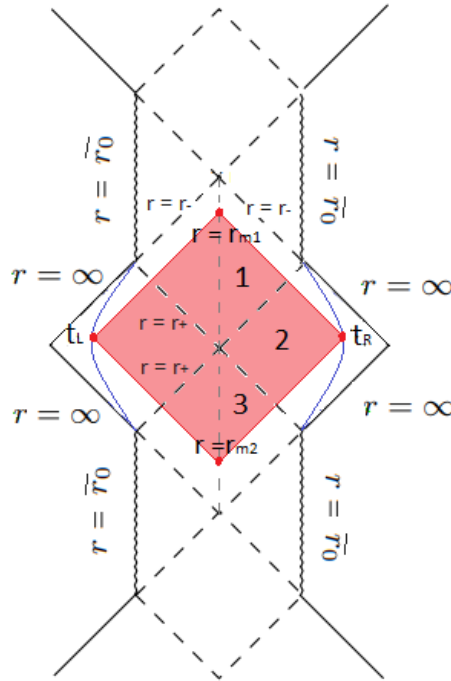


Figure 6: Penrose diagram for the WDW patch in the rotating case.

The definition of the null joints in terms of the tortoise coordinates are:

$$\frac{t_b}{2} + r_\Lambda^* - r^*(r_{m1}) = 0, \quad \frac{t_b}{2} - r_\Lambda^* + r^*(r_{m2}) = 0. \quad (4.33)$$

It will be useful to differentiate with respect to time these expressions to find

$$\frac{dr_{m1}}{dt_b} = \frac{1}{2} \left(\frac{dr^*}{dr_{m1}} \right)^{-1}, \quad \frac{dr_{m2}}{dt_b} = -\frac{1}{2} \left(\frac{dr^*}{dr_{m2}} \right)^{-1}. \quad (4.34)$$

Bulk contributions: We can still split the WDW patch into three regions covering

only the right half of the diagram, which contribute as

$$\begin{aligned} I_{\mathcal{V}}^1 &= \frac{\mathcal{I}}{8G} \int_{r_{m1}}^{r_+} dr \left(\frac{t_b}{2} + r_{\Lambda}^* - r^*(r) \right), & I_{\mathcal{V}}^2 &= \frac{\mathcal{I}}{4G} \int_{r_+}^{\Lambda} dr (r_{\Lambda}^* - r^*(r)), \\ I_{\mathcal{V}}^3 &= \frac{\mathcal{I}}{8G} \int_{r_{m2}}^{r_+} dr \left(-\frac{t_b}{2} + r_{\Lambda}^* - r^*(r) \right). \end{aligned} \quad (4.35)$$

The whole bulk contribution then amounts to

$$\begin{aligned} I_{\mathcal{V}} &= \frac{\mathcal{I}}{2G} \int_{r_+}^{\Lambda} dr (r_{\Lambda}^* - r^*(r)) + \\ &+ \frac{\mathcal{I}}{4G} \left[\int_{r_{m1}}^{r_+} dr \left(\frac{t_b}{2} + r_{\Lambda}^* - r^*(r) \right) + \int_{r_+}^{r_{m2}} dr \left(\frac{t_b}{2} - r_{\Lambda}^* + r^*(r) \right) \right]. \end{aligned} \quad (4.36)$$

The rate of the bulk action is

$$\frac{dI_{\mathcal{V}}}{dt_b} = \frac{\mathcal{I}}{8G} (r_{m2} - r_{m1}), \quad (4.37)$$

where the relations (4.33) are used to obtain a vanishing result when differentiating the ends of integration. The result simplifies when performing the late time limit, when $r_{m1} \rightarrow r_+$ and $r_{m2} \rightarrow r_-$, and the bulk action time-derivative becomes

$$\lim_{t_b \rightarrow \infty} \frac{dI_{\mathcal{V}}}{dt_b} = -\frac{(\nu^2 + 3)l}{16G} (r_+ - r_-) + \frac{1}{8G} \left(\frac{\kappa}{l} c^2 - \alpha ac \right) (r_+ - r_-). \quad (4.38)$$

Null joint contributions: As in the non-rotating case, the joints at $r = \Lambda$ give a time-independent contribution, and then they are not of interest to find the rate of complexity. We have two time-dependent contributions coming from the top and bottom joints.

As a function of r , these contributions are proportional to:

$$\mathbf{a} = \eta \log \left| A^2 \frac{1}{2} u^\alpha v_\alpha \right| = \eta \log \left| \frac{A^2}{l^2} \frac{r \Psi(r)}{(\nu^2 + 3)(r - r_-)(r - r_+)} \right|. \quad (4.39)$$

For $r = r_{m1}$ and $r = r_{m2}$ we have to insert respectively $\eta_1 = -1$ and $\eta_2 = 1$.

The action of each joint then is:

$$I_{\mathcal{J}}^k = \pm \frac{1}{4G} \sqrt{\frac{r_k}{4} \Psi(r_k)} \log \left| \frac{l^2}{A^2} F(r_k) \right|, \quad F(r_k) \equiv \frac{(\nu^2 + 3)(r_k - r_-)(r_k - r_+)}{r_k \Psi(r_k)}, \quad (4.40)$$

where the + sign is for the joint 1 and the - for the joint 2 and $r_1 = r_{m1}$, $r_2 = r_{m2}$. We differentiate with respect to time the null joint contributions:

$$\begin{aligned} \frac{dI_{\mathcal{J}}^k}{dt_b} &= \pm \frac{l}{8G} \frac{dr_k}{dt_b} \left\{ \sqrt{r_k \Psi(r_k)} \frac{d}{dr_k} \left(\log \left| \frac{l^2}{A^2} F(r_k) \right| \right) + \right. \\ &\left. + \frac{1}{2} \frac{6(\nu^2 - 1)r_k + (\nu^2 + 3)(r_+ + r_-) - 4\nu \sqrt{(\nu^2 + 3)r_+ r_-}}{\sqrt{r_k \Psi(r_k)}} \log \left| \frac{l^2}{A^2} F(r_k) \right| \right\}, \end{aligned} \quad (4.41)$$

where again the + sign is for the joint 1 and the - for the joint 2. Using eqs. (4.34) in the previous expression, it is possible to find the complete time dependence of the null contributions. In the late-time limit, we find:

$$\lim_{t_b \rightarrow \infty} \frac{dI_{\mathcal{J}}^k}{dt_b} = \frac{(\nu^2 + 3)l}{16G} (r_+ - r_-), \quad k = 1, 2. \quad (4.42)$$

Total: Summing all the previous asymptotic expressions, the late-time limit of the action growth is:

$$\lim_{t_b \rightarrow \infty} \frac{dI}{dt_b} = \frac{(\nu^2 + 3)l}{16G} (r_+ - r_-) - \frac{1}{8G} \left(\frac{\kappa}{l} c^2 - \alpha a c \right) (r_+ - r_-). \quad (4.43)$$

Taking into account eq. (2.22) we finally find:

$$\lim_{t_b \rightarrow \infty} \frac{1}{l} \frac{dI}{dt_b} = \lim_{\tau \rightarrow \infty} \frac{dI}{d\tau} = \frac{(\nu^2 + 3)}{16G} (r_+ - r_-) = TS. \quad (4.44)$$

The late-time limit can be recovered also with the methods introduced in [18] and the results agree; details of the explicit calculation can be found in appendix B.

5 Conclusions

In this paper we investigated the CA conjecture for WAdS BHs realized as solutions of Einstein gravity plus matter. We have found that, both in the rotating and in the non-rotating cases, the asymptotic limit of the action in the WDW patch is:

$$\lim_{\tau \rightarrow \infty} \frac{dI}{d\tau} = TS, \quad TS = \frac{(r_+ - r_-)(3 + \nu^2)}{16G}. \quad (5.1)$$

In the rotating case, the only terms which contribute are the bulk and the joints term, while in the non-rotating case there is also a surface GHY contribution. Although the details of the calculation are quite different, the final result is a continuous function of the parameters of the solution (r_+, r_-) . A curious feature of the non-rotating case is that there exists an initial time period $(t < t_c)$ in which complexity is constant; this is the same as in the AdS case [22].

The results can be compared to the ones from the CV conjecture, studied in [44]:

$$\lim_{\tau \rightarrow \infty} \frac{dV}{d\tau} = \frac{\pi l}{2} (r_+ - r_-) \sqrt{3 + \nu^2} = TS \frac{8\pi Gl}{\sqrt{3 + \nu^2}}. \quad (5.2)$$

Already in the AdS case the CA conjecture is known to be more universal, because no explicit factor of the curvature l related to the asymptotic of the spacetime is needed. In the case of WAdS, this behavior is confirmed: the CA gives as a result TS , independently from the two parameters (l, ν) which determine the space-time asymptotic, while in the CV a factor $\frac{\sqrt{3+\nu^2}}{8\pi Gl}$ should be inserted in front of the volume in order to match with the CA.

WAdS BHs can be realized also as solutions of TMG (Topological Massive Gravity) and NMG (New Massive Gravity). It would be interesting to study both CA and CV in these examples, in order to get control on both the conjectures in the case of higher derivatives terms in the gravity action. The CA conjecture for higher derivatives gravity was already studied by several authors in [60, 61, 62, 63], but always in the late-time limit. In particular, ref. [62] studied the late-time limit of CA conjecture for WAdS BHs in TMG; the asymptotic growth of the action is not proportional to TS .

Another important open problem is to study complexity from the field theory dual. In particular, it would be interesting to generalize the Liouville action [13, 14] approach to WAdS.

Appendix

A Comparison with ref. [45].

Let us fix the couplings (κ, L, α) in the action (2.16); the field equation determine the solution parameters (ν, l) as follows:

$$\nu^2 + \frac{2\kappa}{\alpha L^2}\nu - 3 = 0, \quad \nu = -\frac{\kappa}{\alpha L^2} \pm \sqrt{\frac{\kappa^2}{\alpha^2 L^4} + 3}, \quad l = \frac{\kappa\nu}{\alpha}. \quad (\text{A.1})$$

Note that the following transformation on the couplings and fields gives an invariance of the action (2.16):

$$\kappa \rightarrow -\kappa, \quad \alpha \rightarrow -\alpha, \quad A_\mu \rightarrow iA_\mu. \quad (\text{A.2})$$

This is just a formal trick, because the gauge field becomes imaginary. This is useful in order to match with the results of [45], because they consider just the $\kappa = 1$ case.

The metric used in [45] reads:

$$ds^2 = pd\tilde{t}^2 + \frac{d\tilde{r}^2}{h^2 - pq} + 2hd\tilde{t}d\tilde{\theta} + qd\tilde{\theta}^2, \quad (\text{A.3})$$

We can put the metric (2.1) in the form (A.3) by means of the coordinate transformations:

$$\tilde{t} = \sqrt{\frac{l^3}{\omega}}t, \quad \tilde{r} = r - \frac{\sqrt{r_+r_-(\nu^2 + 3)}}{2\nu}, \quad \tilde{\theta} = -\frac{\sqrt{\omega l^3}}{2}\theta, \quad (\text{A.4})$$

where

$$\omega = \frac{\nu^2 + 3}{2l} \left((r_+ + r_-) - \frac{\sqrt{r_+r_-(\nu^2 + 3)}}{\nu} \right). \quad (\text{A.5})$$

Let us introduce

$$\begin{aligned} \gamma^2 &= \frac{l}{\omega} \frac{3(1 - \nu^2)}{3 - \nu^2}, \quad \mu = \frac{\omega}{8Gl}, \\ 4G\mathcal{J} &= (-\kappa) \frac{2\nu(r_+ + r_-)\sqrt{r_+r_-(\nu^2 + 3)} - (5\nu^2 + 3)r_+r_-}{2l \left(\nu(r_+ + r_-) - \sqrt{r_+r_-(\nu^2 + 3)} \right)}. \end{aligned} \quad (\text{A.6})$$

The quantity γ^2 is negative for $\nu > 1$. The functions appearing in the metric (A.3) then are:

$$p(\tilde{r}) = 8G\mu, \quad h(\tilde{r}) = -2\frac{\nu}{l}\tilde{r}, \quad q(\tilde{r}) = -2\frac{\gamma^2}{L^2}\tilde{r}^2 + 2\tilde{r} - \frac{4G\mathcal{J}}{\alpha}. \quad (\text{A.7})$$

Only the linear part in \tilde{r} of the $U(1)$ gauge field $A_{\tilde{\theta}}$ is determined by the equations of motion:

$$A_{\tilde{\theta}}(\tilde{r}) = E \mp \frac{2\gamma}{L\sqrt{\kappa}}\tilde{r}, \quad (\text{A.8})$$

The constant part, denoted by E , does not enter both the equations of motion and the calculation of the action, so we ignore it. Moreover, the \mp sign in eq. (A.8) should be taken in correspondence of the \pm sign of the second equation in (2.21).

The constant value of $A_{\tilde{t}}$ is not determined by the equations of motion, but affects the value of the bulk part of the action. In the $\kappa = 1$ case, it can be extracted from [45]:

$$A_{\tilde{t}}(\tilde{r}) = \frac{\alpha^2 L^2 - 1}{\gamma\alpha L} + \zeta, \quad A_t = \frac{d\tilde{t}}{dt}A_{\tilde{t}} = -\frac{l}{\nu}\sqrt{\frac{3}{2}}\sqrt{1 - \nu^2} + \zeta\sqrt{\frac{l^3}{\omega}}. \quad (\text{A.9})$$

The value of ζ affects the way in which the physical mass is associated to the Killing vector $\partial/\partial t$; gauge invariance of the result is recovered by $\zeta = 0$. For $\kappa = -1$, we can use the symmetry (A.2) to match with [45]. This gives the gauge field A_t :

$$A_t = a = \frac{l}{\nu} \sqrt{\frac{3}{2}} \sqrt{\nu^2 - 1} + \zeta \sqrt{\frac{l^3}{\omega}}, \quad (\text{A.10})$$

which reduces to eq. (2.22) for $\zeta = 0$.

B Another way to compute the asymptotic growth of action

The asymptotic growth of the action of the WDW patch can be computed also in the way introduced in [18]. This is a cross-check of our calculation.

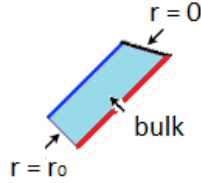


Figure 7: Asymptotic contributions for the non-rotating case.

Non-rotating case: The relevant region in the WDW patch is shown in figure 7. The time derivative of the bulk contribution is given by (4.22). The time derivative of the GHY term nearby the singularity is given by eq. (4.24). The contribution from the joint at $r = r_m$ is replaced by the GHY term nearby the horizon:

$$\Delta I_{\text{GHY}}^{r_0} = \frac{(\nu^2 + 3)l}{16G} \Delta t_b [2r - r_0]_{r=r_0}, \quad (\text{B.1})$$

which in the asymptotic limit gives the same contribution as the null joint.

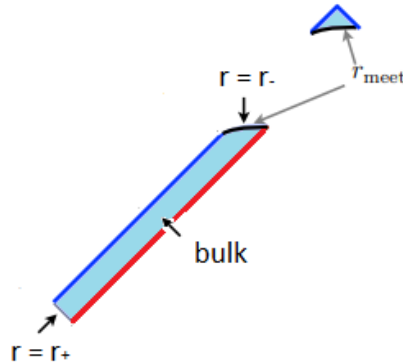


Figure 8: Asymptotic contributions for the rotating case.

Rotating case: The region is depicted in figure 8. The bulk contribution is still given by eq. (4.38). The two null joints contributions are replaced by the GHY term evaluated

on two constant- r surfaces, one at $r \approx r_-$ and one at $r \approx r_+$. The induced metric on these constant- r surfaces is:

$$h_{ij} = l^2 \begin{pmatrix} 1 & \nu r - \frac{1}{2} \sqrt{(3 + \nu^2)r_+ r_-} \\ \nu r - \frac{1}{2} \sqrt{(3 + \nu^2)r_+ r_-} & \frac{r}{4} \Psi(r) \end{pmatrix}, \quad (\text{B.2})$$

$$\sqrt{h} = \frac{l^2}{2} \sqrt{(\nu^2 + 3)(r_+ - r)(r - r_-)}. \quad (\text{B.3})$$

The normal vector to these slices is

$$n^\mu = \left(0, -\frac{1}{l} \sqrt{(\nu^2 + 3)(r_+ - r)(r - r_-)}, 0 \right), \quad n^\alpha n_\alpha = -1, \quad (\text{B.4})$$

and the extrinsic curvature is

$$K = \frac{\sqrt{\nu^2 + 3}}{2l} \frac{2r - r_+ - r_-}{\sqrt{(r_+ - r)(r - r_-)}}. \quad (\text{B.5})$$

The GHY term nearby the inner horizon gives:

$$\frac{dI_{\text{GHY}}^{r_-}}{dt_b} = -\frac{l}{4} \sqrt{\nu^2 + 3} [2r - r_+ - r_-]_{r=r_-}, \quad (\text{B.6})$$

while the term from the outer horizon

$$\frac{dI_{\text{GHY}}^{r_+}}{dt_b} = \frac{l}{4} \sqrt{\nu^2 + 3} [2r - r_+ - r_-]_{r=r_+}. \quad (\text{B.7})$$

These two contributions give the same result as the asymptotic contributions from the joints.

References

- [1] S. Ryu and T. Takayanagi, Phys. Rev. Lett. **96** (2006) 181602 doi:10.1103/PhysRevLett.96.181602 [[hep-th/0603001](#)].
- [2] H. Casini, M. Huerta and R. C. Myers, JHEP **1105** (2011) 036 doi:10.1007/JHEP05(2011)036 [[arXiv:1102.0440](#) [hep-th]].
- [3] A. Lewkowycz and J. Maldacena, JHEP **1308** (2013) 090 doi:10.1007/JHEP08(2013)090 [[arXiv:1304.4926](#) [hep-th]].
- [4] J. D. Bekenstein, Phys. Rev. D **7** (1973) 2333. doi:10.1103/PhysRevD.7.2333
- [5] J. M. Bardeen, B. Carter and S. W. Hawking, Commun. Math. Phys. **31** (1973) 161. doi:10.1007/BF01645742
- [6] J. M. Maldacena, JHEP **0304** (2003) 021 doi:10.1088/1126-6708/2003/04/021 [[hep-th/0106112](#)].
- [7] T. Hartman and J. Maldacena, JHEP **1305** (2013) 014 doi:10.1007/JHEP05(2013)014 [[arXiv:1303.1080](#) [hep-th]].
- [8] L. Susskind, [Fortsch. Phys. **64** (2016) 24] Addendum: Fortsch. Phys. **64** (2016) 44 doi:10.1002/prop.201500093, 10.1002/prop.201500092 [[arXiv:1403.5695](#) [hep-th], [arXiv:1402.5674](#) [hep-th]].

- [9] L. Susskind, Fortsch. Phys. **64** (2016) 49 doi:10.1002/prop.201500095 [[arXiv:1411.0690](#) [hep-th]].
- [10] R. Jefferson and R. C. Myers, JHEP **1710** (2017) 107 doi:10.1007/JHEP10(2017)107 [[arXiv:1707.08570](#) [hep-th]].
- [11] S. Chapman, M. P. Heller, H. Marrochio and F. Pastawski, Phys. Rev. Lett. **120** (2018) no.12, 121602 doi:10.1103/PhysRevLett.120.121602 [[arXiv:1707.08582](#) [hep-th]].
- [12] K. Hashimoto, N. Iizuka and S. Sugishita, Phys. Rev. D **96** (2017) no.12, 126001 doi:10.1103/PhysRevD.96.126001 [[arXiv:1707.03840](#) [hep-th]].
- [13] P. Caputa, N. Kundu, M. Miyaji, T. Takayanagi and K. Watanabe, JHEP **1711** (2017) 097 doi:10.1007/JHEP11(2017)097 [[arXiv:1706.07056](#) [hep-th]].
- [14] A. Bhattacharyya, P. Caputa, S. R. Das, N. Kundu, M. Miyaji and T. Takayanagi, [arXiv:1804.01999](#) [hep-th].
- [15] B. Swingle, Phys. Rev. D **86** (2012) 065007 doi:10.1103/PhysRevD.86.065007 [[arXiv:0905.1317](#) [cond-mat.str-el]].
- [16] D. Stanford and L. Susskind, Phys. Rev. D **90** (2014) no.12, 126007 doi:10.1103/PhysRevD.90.126007 [[arXiv:1406.2678](#) [hep-th]].
- [17] A. R. Brown, D. A. Roberts, L. Susskind, B. Swingle and Y. Zhao, Phys. Rev. Lett. **116** (2016) no.19, 191301 doi:10.1103/PhysRevLett.116.191301 [[arXiv:1509.07876](#) [hep-th]].
- [18] A. R. Brown, D. A. Roberts, L. Susskind, B. Swingle and Y. Zhao, Phys. Rev. D **93** (2016) no.8, 086006 doi:10.1103/PhysRevD.93.086006 [[arXiv:1512.04993](#) [hep-th]].
- [19] G. Hayward, Phys. Rev. D **47** (1993) 3275. doi:10.1103/PhysRevD.47.3275
- [20] L. Lehner, R. C. Myers, E. Poisson and R. D. Sorkin, Phys. Rev. D **94** (2016) no.8, 084046 doi:10.1103/PhysRevD.94.084046 [[arXiv:1609.00207](#) [hep-th]].
- [21] S. Chapman, H. Marrochio and R. C. Myers, JHEP **1701** (2017) 062 doi:10.1007/JHEP01(2017)062 [[arXiv:1610.08063](#) [hep-th]].
- [22] D. Carmi, S. Chapman, H. Marrochio, R. C. Myers and S. Sugishita, JHEP **1711** (2017) 188 doi:10.1007/JHEP11(2017)188 [[arXiv:1709.10184](#) [hep-th]].
- [23] Y. Neiman, [arXiv:1212.2922](#) [hep-th].
- [24] K. Parattu, S. Chakraborty, B. R. Majhi and T. Padmanabhan, Gen. Rel. Grav. **48** (2016) no.7, 94 doi:10.1007/s10714-016-2093-7 [[arXiv:1501.01053](#) [gr-qc]].
- [25] R. G. Cai, S. M. Ruan, S. J. Wang, R. Q. Yang and R. H. Peng, JHEP **1609** (2016) 161 doi:10.1007/JHEP09(2016)161 [[arXiv:1606.08307](#) [gr-qc]].
- [26] J. L. F. Barbon and E. Rabinovici, JHEP **1601** (2016) 084 doi:10.1007/JHEP01(2016)084 [[arXiv:1509.09291](#) [hep-th]].
- [27] S. Bolognesi, E. Rabinovici and S. R. Roy, [arXiv:1802.02045](#) [hep-th].
- [28] A. P. Reynolds and S. F. Ross, Class. Quant. Grav. **35** (2018) no.9, 095006 doi:10.1088/1361-6382/aab32d [[arXiv:1712.03732](#) [hep-th]].

- [29] M. Moosa, JHEP **1803** (2018) 031 doi:10.1007/JHEP03(2018)031 [[arXiv:1711.02668](#) [hep-th]].
- [30] M. Moosa, Phys. Rev. D **97** (2018) no.10, 106016 doi:10.1103/PhysRevD.97.106016 [[arXiv:1712.07137](#) [hep-th]].
- [31] S. Chapman, H. Marrochio and R. C. Myers, [arXiv:1804.07410](#) [hep-th].
- [32] S. Chapman, H. Marrochio and R. C. Myers, [arXiv:1805.07262](#) [hep-th].
- [33] B. Swingle and Y. Wang, [arXiv:1712.09826](#) [hep-th].
- [34] Y. S. An and R. H. Peng, Phys. Rev. D **97** (2018) no.6, 066022 doi:10.1103/PhysRevD.97.066022 [[arXiv:1801.03638](#) [hep-th]].
- [35] D. Anninos, W. Li, M. Padi, W. Song and A. Strominger, JHEP **0903** (2009) 130 doi:10.1088/1126-6708/2009/03/130 [[arXiv:0807.3040](#) [hep-th]].
- [36] S. Detournay, T. Hartman and D. M. Hofman, Phys. Rev. D **86** (2012) 124018 doi:10.1103/PhysRevD.86.124018 [[arXiv:1210.0539](#) [hep-th]].
- [37] D. M. Hofman and B. Rollier, Nucl. Phys. B **897** (2015) 1 doi:10.1016/j.nuclphysb.2015.05.011 [[arXiv:1411.0672](#) [hep-th]].
- [38] K. Jensen, JHEP **1712** (2017) 111 doi:10.1007/JHEP12(2017)111 [[arXiv:1710.11626](#) [hep-th]].
- [39] D. Anninos, J. Samani and E. Shaghoulian, JHEP **1402** (2014) 118 doi:10.1007/JHEP02(2014)118 [[arXiv:1309.2579](#) [hep-th]].
- [40] A. Castro, D. M. Hofman and N. Iqbal, JHEP **1602** (2016) 033 doi:10.1007/JHEP02(2016)033 [[arXiv:1511.00707](#) [hep-th]].
- [41] T. Azeanagi, S. Detournay and M. Riegler, [arXiv:1801.07263](#) [hep-th].
- [42] W. Song, Q. Wen and J. Xu, Phys. Rev. Lett. **117** (2016) no.1, 011602 doi:10.1103/PhysRevLett.117.011602 [[arXiv:1601.02634](#) [hep-th]].
- [43] W. Song, Q. Wen and J. Xu, JHEP **1702** (2017) 067 doi:10.1007/JHEP02(2017)067 [[arXiv:1610.00727](#) [hep-th]].
- [44] R. Auzzi, S. Baiguera and G. Nardelli, [arXiv:1804.07521](#) [hep-th].
- [45] M. Banados, G. Barnich, G. Compere and A. Gomberoff, Phys. Rev. D **73** (2006) 044006 doi:10.1103/PhysRevD.73.044006 [[hep-th/0512105](#)].
- [46] K. A. Moussa, G. Clement and C. Leygnac, Class. Quant. Grav. **20** (2003) L277 doi:10.1088/0264-9381/20/24/L01 [[gr-qc/0303042](#)].
- [47] A. Bouchareb and G. Clement, Class. Quant. Grav. **24** (2007) 5581 doi:10.1088/0264-9381/24/22/018 [[arXiv:0706.0263](#) [gr-qc]].
- [48] M. Banados, C. Teitelboim and J. Zanelli, Phys. Rev. Lett. **69** (1992) 1849 doi:10.1103/PhysRevLett.69.1849 [[hep-th/9204099](#)].
- [49] M. Banados, M. Henneaux, C. Teitelboim and J. Zanelli, Phys. Rev. D **48** (1993) 1506 Erratum: [Phys. Rev. D **88** (2013) 069902] doi:10.1103/PhysRevD.48.1506, 10.1103/PhysRevD.88.069902 [[gr-qc/9302012](#)].

- [50] D. Anninos, JHEP **0909** (2009) 075 doi:10.1088/1126-6708/2009/09/075 [arXiv:0809.2433 [hep-th]].
- [51] G. Clement, Class. Quant. Grav. **26** (2009) 105015 doi:10.1088/0264-9381/26/10/105015 [arXiv:0902.4634 [hep-th]].
- [52] E. Tonni, JHEP **1008** (2010) 070 doi:10.1007/JHEP08(2010)070 [arXiv:1006.3489 [hep-th]].
- [53] G. Compere, S. Detournay and M. Romo, Phys. Rev. D **78** (2008) 104030 doi:10.1103/PhysRevD.78.104030 [arXiv:0808.1912 [hep-th]].
- [54] S. Detournay and M. Guica, JHEP **1308** (2013) 121 doi:10.1007/JHEP08(2013)121 [arXiv:1212.6792 [hep-th]].
- [55] P. Karndumri and E. O. ColgÄain, JHEP **1310** (2013) 094 doi:10.1007/JHEP10(2013)094 [arXiv:1307.2086 [hep-th]].
- [56] M. Gurses, Class. Quant. Grav. **11** (1994) no.10, 2585. doi:10.1088/0264-9381/11/10/017
- [57] G. Barnich and G. Compere, Phys. Rev. Lett. **95** (2005) 031302 doi:10.1103/PhysRevLett.95.031302 [hep-th/0501102].
- [58] F. Jugeau, G. Moutsopoulos and P. Ritter, Class. Quant. Grav. **28** (2011) 035001 doi:10.1088/0264-9381/28/3/035001 [arXiv:1007.1961 [hep-th]].
- [59] S. Lloyd, Nature 406 (2000), no. 6799 1047-1054.
- [60] M. Alishahiha, A. Faraji Astaneh, A. Naseh and M. H. Vahidinia, JHEP **1705** (2017) 009 doi:10.1007/JHEP05(2017)009 [arXiv:1702.06796 [hep-th]].
- [61] W. D. Guo, S. W. Wei, Y. Y. Li and Y. X. Liu, Eur. Phys. J. C **77** (2017) no.12, 904 doi:10.1140/epjc/s10052-017-5466-5 [arXiv:1703.10468 [gr-qc]].
- [62] M. Ghodrati, Phys. Rev. D **96** (2017) no.10, 106020 doi:10.1103/PhysRevD.96.106020 [arXiv:1708.07981 [hep-th]].
- [63] M. M. Qaemmaqami, Phys. Rev. D **97** (2018) no.2, 026006 doi:10.1103/PhysRevD.97.026006 [arXiv:1709.05894 [hep-th]].